

**CREEP CHARACTERISTICS OF AUSTENITIC STAINLESS STEEL FOILS
UNDER OXIDATIVE AND NON-OXIDATIVE ENVIRONMENT**

FATIMAH MOHAMMED KADHIM

UNIVERSITI TEKNOLOGI MALAYSIA

CREEP CHARACTERISTICS OF AUSTENITIC STAINLESS STEEL FOILS
UNDER OXIDATIVE AND NON-OXIDATIVE ENVIRONMENT

FATIMAH MOHAMMED KADHIM

A project report submitted in partial fulfilment of the
requirements for the award of the degree of
Master of Engineering (Mechanical)

Faculty of Mechanical Engineering
Universiti Teknologi Malaysia

JANUARY 2015

Dedicated to

*My dearest country **IRAQ***

*My parents, **Mohammed Kadhim (Late)** and **Hekma Attallah**,*

*My respected supervisor **Professor Dr Mohd Nasir Tamin***

*All my family and friends for their immeasurable support and love throughout my
journey for education.*

ACKNOWLEDGEMENT

In the name of ALLAH, the most gracious and the most merciful, Who has taught man what he did not know. The completion of this research was not possible without His help and mercy. HE is the one who knows the hardships and HE is the one I seek HIS satisfaction and ask HIS acceptance.

I would like to express my deepest gratitude towards my supervisor, Professor Dr. Mohd Nasir Tamin for his guidance, encouragement and valuable comments during the research and writing of this thesis. His attention and technical expertise was key elements to my success. I am satisfied in gaining an in depth knowledge from him.

I wish to express my appreciation to my Computational and Solid Mechanics (CSM) - lab members for their generous cooperation, hospitality, time and insight on related matters during this research. Also thank you to Ali Farokhi Nejad for helping and assisting in running the experiment. The experimental work would not have been possible without the help from you.

Special thank goes to my parents, Mohammed Kadhim and Hekma Attallah and family members for their patience and sacrifice during my academic career. Their concern, encouragement, moral and financial support over the years has always been a source of motivation that enables me to achieve this degree.

Last but not the least, Thank Allah until you are satisfied and after satisfaction first and foremost.

ABSTRACT

Compact and high efficiency recuperator with thin foil corrugated air cell as the primary surface is employed in clean and efficient microturbine system (100 kW). Current primary surface recuperators are made of AISI 347 austenitic stainless steel foils that operate at gas inlet temperature of less than 650 °C and attain approximately 30 percent of efficiency. Efficiency of greater than 40 percent is possible with the increase in turbine inlet temperature to 1230 °C, and as a result recuperator inlet temperature increase to 843 °C. This study establishes base line creep rupture behaviour of AISI 347 austenitic stainless steel foils at operating temperature of 700 °C and applied stresses of 150,182 and 221 MPa in air as oxidation environment, and in inert gas (Argon gas) as non-oxidation environment. Creep behaviour of the foil shows that the primary creep stage is short and creep life of the foil is dominated by secondary and tertiary creep deformation. The time to rupture for the foil specimen is 78 hours with the corresponding rupture strain of 18.42 percent in air and 102 hours with the corresponding rupture strain of 15 percent in Argon gas for the applied stresses of 150,182 and 221 MPa at 700 °C. Creep curves for AISI 347 austenitic stainless steel foil at 700 °C and at 150,182 and 221 MPa are well represented by the modified Theta-Projection concept model with hardening and softening terms. The creep coefficients, θ_1 and θ_3 , and the exponent α are 0.0355, 0.04645 and 1.39 respectively in air and 0.0035, 0.048 and 1.3 respectively in Ar gas environment. Theta-Projection parameter values of the creep curves at temperature of 700 °C and applied stress of range 150,182 and 221 MPa shows a sudden gradient change at applied stress of 150 MPa possibly due to different mechanism of dislocation movements and microstructure changes. The creep curves for AISI 347 austenitic stainless steel foil at 700 °C and at 150,182 and 221 MPa in inert gas are represented by the power-law model and parameters of this model A , n and Q are $7.947(10^{10})$, 1.73 and 556.4KJ/mol., respectively. Two different creep failure mechanisms for austenitic stainless steel foils are possible since the creep failure data falls very close to the boundary of dislocation and diffusion creep regions in the creep mechanism map for bulk material. Morphology of fractured foil surface revealed intergranular fracture with shallow network of faceted voids. The formation of creep cavities is significant. Post test phase analysis indicates the formation of carbides, namely $Cr_{23}C_6$, NbC and Fe_3Nb_3C .

ABSTRAK

Pemulih padat serta berkecekapan tinggi dengan kerajang tipis sel udara beralun sebagai permukaan utama digunakan dalam sistem mikroturbin bersih dan cekap (100 kW). Pemulih permukaan utama semasa diperbuat daripada AISI 347 kerajang austenit keluli tahan karat yang beroperasi pada suhu gas masuk kurang daripada 650 °C serta mencapai kira-kira 30 peratus kecekapan. Kecekapan yang lebih besar daripada 40 peratus adalah mungkin dengan peningkatan suhu masuk turbin hingga 1230 °C, dan hasilnya suhu masuk pemulih meningkat hingga 843 °C. Kajian ini menetapkan garis asas kelakuan rayapan pecah AISI 347 austenit kerajang keluli tahan karat pada suhu operasi pada 700 °C dan tekanan yang digunakan adalah 150.182 dan 221 MPa dalam udara persekitaran pengoksidaan dan dalam gas lengai (gas Argon) sebagai persekitaran bukan-pengoksidaan. Kelakuan rayapan kerajang menunjukkan bahawa peringkat rayapan utama adalah pendek dan jangka hayat rayapan kerajang dikuasai oleh pengubahbentuk rayapan sekunder dan tertier. Masa untuk pecah bagi spesimen kerajang adalah 78 jam dengan ketegangan kepecahan yang sepadan sebanyak 18.42 peratus di udara dan 102 jam dengan ketegangan kepecahan yang sepadan sebanyak 15 peratus dalam gas Argon. Lengkuk rayapan bagi kerajang austenit keluli tahan karat AISI 347 pada 700 °C, 150,182 dan 221 MPa diwakili dengan menggunakan model konsep Unjuran Theta yang diubah suai daripada segi pengerasan dan pelembutan. Pekali rayapan, θ_1 dan θ_3 , dan α eksponen adalah 0,0355, 0,04645 dan 1.39 masing-masing di udara dan 0,0035, 0,048 dan 1.3 masing-masing dalam gas lengai. Nilai parameter-parameter Unjuran Theta rayapan eksperimen pada suhu 700 °C dan tekanan digunakan daripada julat 150,182 dan 221 MPa menunjukkan perubahan secara tiba-tiba pada kecerunan tekanan gunaan pada 150 MPa mungkin disebabkan oleh mekanisma yang berbeza daripada pergerakan kehelan dan perubahan-perubahan mikrostruktur dan juga lengkuk rayapan bagi kerajang austenit keluli tahan karat AISI 347 pada 700 °C, 150,182 dan 221 MPa dalam gas lengai diwakili oleh model kuasa-hukum dan parameter-parameter model ini adalah A, n dan Q iaitu masing-masing $[7,947 * 10^7]$ ^ 10, 1.73 dan 556.4KJ/mol. Dua mekanisme kegagalan rayapan yang berbeza bagi austenit kerajang keluli tahan karat adalah mungkin kerana data kegagalan rayapan berada sangat dekat dengan sempadan kehelan dan kawasan resapan rayapan dalam peta mekanisme rayapan untuk bahan pukal.

TABLE OF CONTENTS

CHAPTER	TITLE	PAGE
	DECLARATION	ii
	DEDICATION	iii
	ACKNOWLEDGEMENT	iv
	ABSTRACT	v
	ABSTRAK	vi
	TABLE OF CONTENTS	vii
	LIST OF TABLES	x
	LIST OF FIGURES	xi
	LIST OF ABBREVIATIONS	
	LIST OF SYMBOLS	
1	INTRODUCTION	1
	1.1 Background of Study	1
	1.2 Research Objective	7
	1.3 Scope of Study	8
	1.4 Results	9
2	LITERATURE REVIEW	10
	2.1 Introduction	10
	2.2 Austenitic Stainless Steel	12
	2.2.1 Behaviour and Properties	13
	2.3 Creep of Austenitic Stainless Steel	14
	2.3.1 Creep Rupture Deformation	15

2.3.2	Creep Strain Rates	16
2.3.3	Creep Deformation Mechanisms	19
2.3.4	Creep Characteristics of Foils for Recuperator	21
2.4	Creep Models for Austenitic Stainless Steel Foils	22
2.5	Theta-Projection Concept Model	23
2.6	Moisture Content	26
2.7	Closure	28
3	RESEARCH METHODOLOGY	29
3.1	Introduction	29
3.2	Research Approach	29
3.3	Metallurgical Study	31
3.4	Mechanical Testing	32
3.4.1	Tension Test	33
3.4.2	Creep Test	33
3.5	Theta-Projection Concept Model for Creep of Foil	36
3.6	Power-law Model for Steady-State Creep of Foil	37
4	RESULTS AND DISCUSSION	38
4.1	Introduction	38
4.2	Metallurgical Characteristics of AISI 347 Stainless Steel Foils	39
4.2.1	Chemical Composition	39
4.2.2	Microstructure Analysis	40
4.3	Tensile Behaviour of ANSI 347 Stainless Steel Foils	42
4.3.1	Stress-Strain Diagram	42
4.4	Creep Deformation Characteristics of AISI 347 Stainless Steel Foils	43
4.4.1	Theta-Projection Concept Model	44
4.4.2	Creep Failure Mechanisms	49

5	CONCLUSIONS AND RECOMMENDATIONS	55
5.1	Conclusions	55
5.2	Recommendations	56
	REFERENCES	57

LIST OF TABLES

TABLE NO	TITLE	PAGE
2.1	Composition of austenitic stainless steel alloy (wt. %)	22
4.1	Chemical compositions (wt.%) of AISI 347 stainless steel foil and bulk	40
4.2	Values of parameters for Theta-Projection concept model for creep test at 700 °C in Air and in Argon gas	47

LIST OF FIGURES

FIGURE NO	TITLE	PAGE
1.1	Microturbine based CHP System [5]	2
1.2	Microturbine Generation (MTG) Components [8]	3
1.3	Schematic of corrugated air-cell in thin foils primary surface Recuperator [7]	4
1.4	Efficiency as a Function of profile [4]	5
1.5	Microturbine Efficiency as a Function of Recuperator Effectiveness	6
2.1	Illustration of the effect of temperature and stress on creep behavior of alloy	16
2.2	Typical shape of creep curve [27].	17
2.3	(a) Steady state creep rate as a function of applied stress at constant temperature (b) as a function of temperature at constant stress [28]	19
2.4	Deformation mechanism map for AISI 304. [29]	20
2.5	Schematic diagrams of viscoelasticity demonstration on creep [11]	27
3.1	Research framework	30
3.2	Geometry of creep test specimen. Dimensions in mm	32
3.3	INSTRON Universal Testing Machine used for tension test	33
3.4	Creep test set up in air for thin foil specimen	34

3.5	Creep test set up in Argon gas for thin foil specimen	35
3.6	Common trend of Theta-Projection model use with creep data of AISI austenitic stainless steel foils.	36
4.1	Optical micrograph of as-received AISI 347 stainless steel foil.	41
4.2	Stress-strain diagram for AISI 347 stainless steel foil at room temperature	42
4.3	Creep curves of AISI 347 foil at 700 °C and 182 MPa in Air and Argon gas	43
4.4	Creep curves of AISI austenitic stainless steel foil at 700 °C at different stresses 150,182 and 221 MPa in air and in Argon gas	44
4.5	Theta-Projection models fitting for the creep rupture test at different stress levels at temperature of 700 °C in Air and in Argon gas .	46
4.6	SEM micrograph of fracture surface morphology of creep foil at 700 °C and 182 MPa in Air	49
4.7	SEM micrograph of fracture surface morphology of creep foil at 700 °C and 182 MPa in Argon gas.	50
4.8	SEM micrographs AISI 347 foil after creep test at 700 °C, 182MPa.(a,b) in air, (d,e) in argon. (c and f) SEM micrographs. White Arrow shows creep cavitation at the junction of grain boundaries	52
4.9	EDx identification of chromium carbide, Cr ₂₃ C ₆ and niobium carbide, NbC In air (b) In Argon	53
4.10	SEM micrographs of cross-section for foil specimen tested at 700 °C at different stress levels in Argon gas	54

LIST OF ABBREVIATIONS

AISI	-	American Iron and Steel Institute
ASME	-	American Society of Mechanical Engineers
ASTM	-	American Society for Testing and Materials
CHP	-	Combined Heat and Power
DG	-	Distributed Generation
EDX	-	Energy Dispersive X-ray Spectroscopy
FESEM	-	Field Emission Scanning Electron Microscope
HHV	-	Higher Heating Value
LVDT	-	Linear Variable Differential Transformer
MTG	-	Microturbine Generation
PID	-	Proportional-Integral-Derivative

LIST OF SYMBOLS

ϵ_0	-	Instantaneous strain
ϵ_{cr}	-	Creep strain
$\epsilon_{primary}$	-	Primary creep
ϵ_t	-	Total strain
$\epsilon_{tertiary}$	-	Tertiary creep
$\dot{\epsilon}_{ss}$	-	Strain rate
t	-	time
T	-	Operating temperature
T_m	-	Melting temperature
wt. %	-	Weight percentage
α	-	Rate constant
θ_1, θ_3	-	Parameters describing the primary and tertiary stages
θ_2, θ_4	-	Rate parameters characterize the curvature of the primary and tertiary stages
n	-	Creep exponent
A	-	Creep coefficient
Q	-	The activation energy for creep
R	-	The gas constant, R = 8.314 J/mol.K

CHAPTER 1

INTRODUCTION

1.1 Background of Study

Distributed Generation (DG) is expected to play an important role in the electric power system in the near future. The insertion of DG systems into existing electric systems has a great impact on real-time system operation and planning. It is widely accepted that Microturbine Generation (MTG) systems are currently attracting much attention for meeting customers' needs in the distributed-powergeneration market. The challenges facing the power industries companies are to provide clean, efficient, affordable and reliable heat and power supplies. Microturbines with their compact size, modularity and potential for relatively low cost, efficient and clean operations are emerging as a leading candidate meeting these needs.

Microturbines are suitable for distributed generation applications due to their flexibility in connection methods, ability to be stacked in parallel to serve larger loads, ability to provide stable and reliable power, and low emissions. Microturbines run at high speed and can be used either in power-only generation or in combined heat and power (CHP) systems. The size range for microturbines currently available

and in development is from 30 to 250 kilowatts (kW), while conventional gas turbine sizes range from 500 kW to 250 megawatts (MW) [1].

Single-shaft microturbine based generation system [2, 6] Figure 1.1 shows the basic components of a microturbine generation system consist of a compressor, turbine, recuperator, high speed generator and power electronics interface. Microturbines, like large gas turbines, operate based on the thermodynamic cycle known as the Brayton cycle [2]. In this cycle, a) the inlet air is compressed in a radial (or centrifugal) compressor, b) fuel is mixed with the compressed air in the combustor and burned, and c) the hot combustion gas is then expanded in the turbine section producing rotating mechanical power to drive the compressor and the electric generator, mounted on the same shaft.

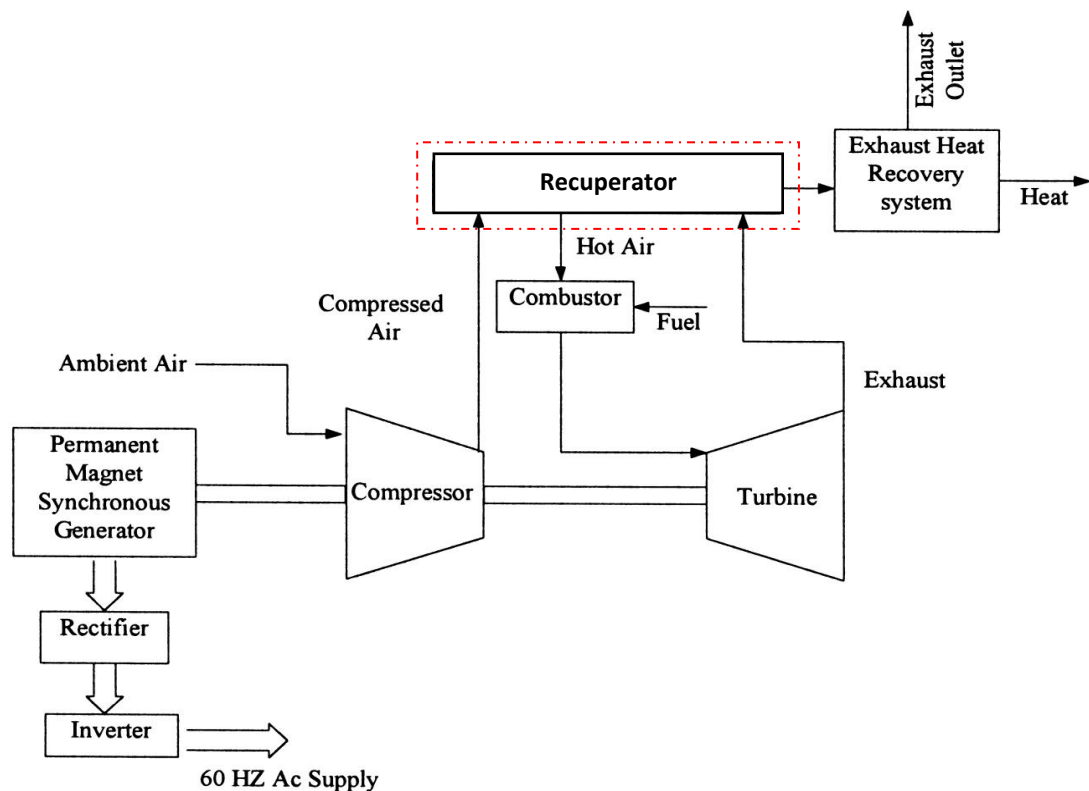


Figure 1.1 Microturbine based CHP System [5]

In a typical microturbine, an air- to- gas heat exchanger (called a recuperator) is added to increase the overall efficiency. The recuperator uses the heat energy available in the turbine's hot exhaust gas to preheat the compressed air before the compressed air goes into the combustion chamber, thereby reducing the fuel needed during the combustion process.

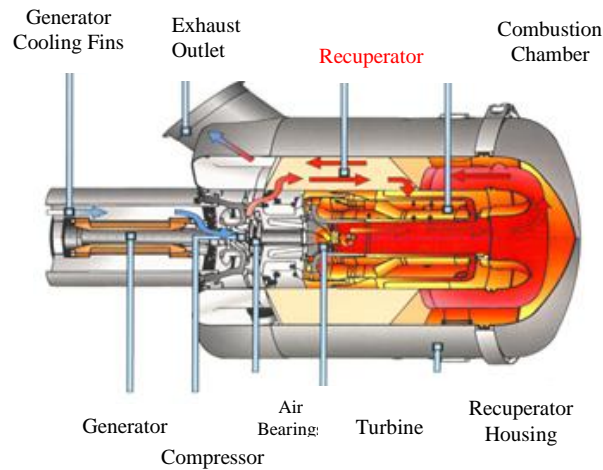


Figure 1.2 Microturbine Generation (MTG) Components [8]

Clean and efficient microturbine system (100 KW) employs compact, high efficiency heat-exchanger or recuperator with thin-foil folded air cell as the primary surface [7]. Figure 1.3 illustrates the corrugated air cell construction in a typical recuperator. The corrugated pattern of the cell maximizes the primary surface area that is in direct contact with turbine exhaust gas on one side and compressor discharge air on the other.

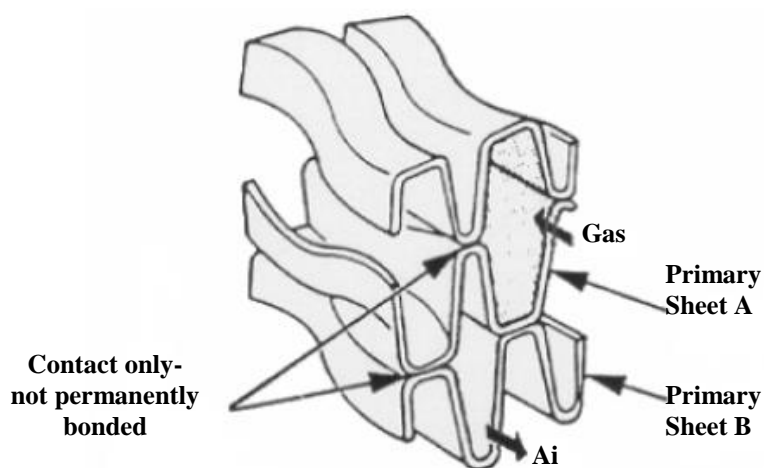


Figure 1.3 Schematic of corrugated air-cell in thin foils primary surface recuperator [7]

Combined heat and power system efficiency of a microturbine is a function of the exhaust heat temperature. Recuperator effectiveness strongly influenced by the microturbine exhaust temperature. Effectiveness in heat exchanger industry is for ratio of the actual heat transferred to the maximum achievable. Most microturbines include built in recuperator. The inclusion of a high effectiveness (90 percent) recuperator essentially doubles the efficiency of a microturbine with a pressure ratio of 3.2, from about 14 percent to about 29 percent depending on component details [1]. With the addition of the recuperator, a microturbine can be suitable for intermediate duty or price-sensitive base load service.

The efficiency of heat exchanger or recuperator depends on arranging and profile since the efficiency increase with increase surface area that clear in figure 1.4.

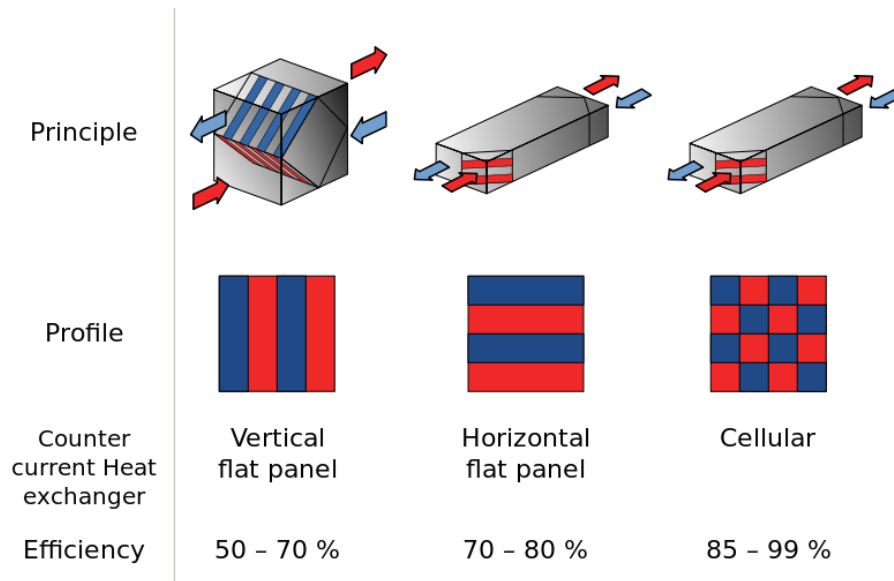


Figure 1.4 Efficiency as a Function of profile [4]

Current primary surface recuperators are made of AISI 347 stainless steel foils that operate at gas inlet temperatures of less than 650 °C and attain about 30 percent efficiency [8]. Efficiency target of greater than 40 percent is possible for low compression ratios such as 5, with the increase in turbine inlet temperature to 1230 °C, and consequently recuperator inlet to 843 °C. At this elevated temperature level, the steel foils are susceptible to creep failure due to the fine grain size, accelerated oxidation due to moisture in the hot exhaust gas and loss of ductility due to the thermal aging. Severe creep deformation able to restrict gas flow, increase recuperator back-pressure and decrease overall efficiency.

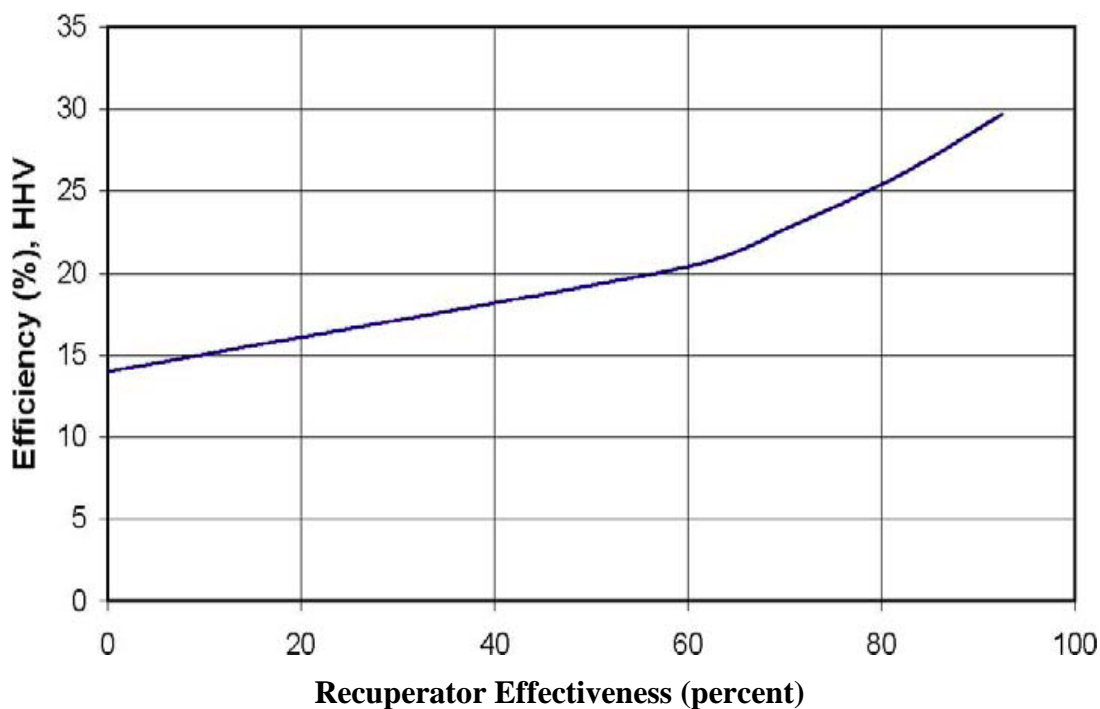


Figure 1.5 Microturbine Efficiency as a Function of Recuperator Effectiveness

Creep deformation is mutually accommodated by a combination of elastic deformation, localized plastic deformation, non-uniform creep, grain boundary sliding and diffusion flow through the grains, along grain and free surfaces [8]. The second phase particles are also responsible for cavity production which leads to intergranular failures [9]. The most important and major step in developing recuperators with upgraded performance is to characterize the current technology. combination of oxidation and corrosion behaviour, and tensile and creep strengths determine the upper temperature and useful lifetime limits. In this respect, creep tests on commercial AISI Type 347 steel recuperator stock has been conducted [6]. Aging effects on the steel up to 30,000 hours above 700 °C has been established in terms of detrimental sigma phase formation [7].

Properties and behavior of AISI 347 steel is generally known for processing and fabrication into high-temperature components such as heat-exchanger piping and gas turbine parts. However, information on these alloys fabricated into thin foils (0.1 – 0.25 mm-thick) for use in primary surface recuperators is limited or nonexistent.

Austenitic stainless steels are among the most widely used alloys for components operating in high temperature environment, in heat exchanger or recuperator and nuclear reactors. It is characterized by a minimum of 10.5 wt % Cr in order to form a passive Cr₂O₃ layer which protects the metal from further corrosion. Austenitic stainless steels also have additions of Ni to stabilize the austenite phase with a face centered cubic (FCC) crystal structure.

The combination of high temperature air and significant water vapor is common in energy generation devices such as, for example, gas turbines, steam turbines, and fuel cells, and in heat exchangers and recuperators handling the gas streams used or generated by such energy generation devices, as well as in equipment for treating, processing, or extracting chemicals or minerals at high temperatures. Accordingly, parts of such devices subjected to these conditions have been fabricated from a variety of austenitic stainless steels.

1.2 Research Objectives

The main objective of this study is to establish baseline creep characteristic and deformation mechanisms of AISI 347 austenitic stainless steel foils in air and in inert gas (Argon gas) at elevated stress (150,182 and 221 MPa) and 700°C through the following tasks:

- a) To establish tensile stress-strain diagram of the foil at room temperature.
- b) To establish creep curve of foil at 700°C and (150,182 and 221 MPa).
- c) To determine creep model for the foil based on Theta projection concept and power-law model.
- d) To identify creep mechanism of the foil.

1.3 Scope of Study

The study covers for AISI 347 austenitic stainless steel foils with thickness of 0.25 mm. Microstructure and chemical composition analysis are performed on the as-received foil. Tension tests of the foil are conducted at room temperature. Creep tests are performed in laboratory air environment at isothermal temperature of 700 °C and non-oxidation environment (inert gas) at isothermal temperature of 700 °C. The applied stress are (150,182 and 221) MPa. Fractographic study is carried out on the fractured foil specimen. Theta projection concept model and power law creep model are executed for describing the long-term creep deformation behaviour of the foils.

1.4 Results

(Creep curves and models) set the baseline creep response of austenitic stainless steel foils at elevated temperatures and stresses can be used to advance the alloy for higher temperature applied with new composition metallurgy.

High efficiency heat exchangers are being developed for new distributed power technology systems particularly microturbines system. Recuperator is the part of microturbines that is responsible for a significant fraction of overall efficiency. Recuperators often require thin-section of austenitic stainless steels operating at elevated temperature ranges up to 800 °C. Most of the recuperators used austenitic stainless steel of Type 347 because of its oxidation resistance properties and competitive cost. At high temperatures which above 650 °C with the presence of moisture environment of the turbine exhaust gas, the material is susceptible to creep and oxidation. These will cause fouling and structural deterioration and leaks, rapidly reducing the effectiveness and life of the recuperator. Therefore the study is

to establish creep characteristics and deformation mechanisms of AISI Type 347 austenitic stainless steel foils at 700 °C and (150,182 and 221) MPa in air and inert gas.

REFERENCES

1. Shah, R.K. *Compact Heat Exchangers for Microturbines*. in *Micro GasTurbines*. 2005. Neuilly-sur-Seine, France: RTO.
2. Goldstein L., Hedman B., Knowles D., Freedman S. I., Woods R., and Schweizer T. 2003. *Gasfired Distributed Energy Resource Technology Characterizations*. National Renewable Energy Laboratory, NREL/TP-620-34783.
3. Lasseter R. 2001. Dynamic Models for Micro-Turbines and Fuel Cells. *Proc. IEEE PES Summer Meeting*, Vancouver, BC, Canada, vol. 2, pp. 761–766.
4. Puttgen H. B., Macgregor P. R., and Lambert F. C. 2003. Distributed Generation: Semantic Hype or the Dawn of A New Era. *IEEE Power and Energy Magazine*, vol. 1, no. 1, pp. 22–29.
5. Malmquist A. 1999. *Analysis of a Gas Turbine Driven Hybrid Drive System for Heavy Vehicles*, Ph.D. Dissertation, School of Electrical Engineering and Information Technology, KTH, Stockholm, Sweden.
6. Malmquist A., Aglen O., Keller E., Suter M., and Wickstrom J. 2000. Microturbines: Speeding the Shift to Distributed Heat and Power. *ABB Review*, no. 3, pp. 22–30.
7. Aquaro, D. and M. Pieve, 2007. Compact Heat Exchangers Optimization Developing a Model for the Thermal-Fluid Dynamic Sizing. *Heat Technology* 25: p. 9-18.
8. Edgar Lara-Curzio R. T. K. M. P. M. a. B. 2004. Screening and Evaluation of Materials for Microturbine Recuperators. in *Proceedings of ASME Turbo Expo 2004 Power for Land, Sea and Air*, Vienna, Austria,.

9. McDonald C.F. 1996. Heat Recovery Exchanger Technology for Very Small Gas Turbines. *International Journal of Turbo and jet Engines*, vol. 13, pp. 239-261.
10. Karen, Pavel; McArdle, Patrick; Takats, Josef. 2014. Toward a Comprehensive Definition of Oxidation State (IUPAC Technical Report). *Pure and Applied Chemistry*. 86
11. Mahmoud Sayed-Ahmed, Khaled Sennah, *Effect of Temperature and Relative Humidity on Creep Deflection for Permanent Wood Foundation Panels*, Department of Civil Engineering, Ryerson University, Toronto, Ontario, Canada.
12. Michael P. Brady, Bruce A. Pint, Knoxville, Philip J. Maziasz, Yukinori Yamamoto, Zhao P. Lu, *Oxidation Resistant High Creep Strength Austenitic Stainless Steel Oak Ridge*, TN (US).
13. Osman H., *Creep Rupture Behavior of AISI 347 Austenitic Stainless Steel Foils at Different Temperature and Stress Levels*, Universiti Teknologi Malaysia, Johor, Malaysia, 2011.
14. McDonald, C.F., 2003. Recuperator Considerations for Future Higher Efficiency Microturbines. *Applied Thermal Engineering*, 23(12): p. 1463-1487.
15. Massardo, A.F., C.F. McDonald, and T. Korakianitis. 2002. Microturbine/Fuel-Cel Coupling for High-Efficiency Electrical-Power Generation. *Journal of Engineering for Gas Turbines and Power*, 124(1): p. 110-116.
16. Ward, M.E., *Primary Surface Recuperator Durability and Applications*, in *Turbomachinery Technology Seminar 1995*: San Diego, CA. p. 395.
17. Young, R. and P. Lovell, *Introduction to Polymers*. Cheltenham. 1991, Cheltenham, UK: Stanley Thornes (Publishers) Ltd.
18. C.F. McDonald, 1996. Heat Recovery Exchanger Technology for Very Small Gas Turbines. *International Journal of Turbo and jet Engines*, vol. 13, pp. 239-261.
19. Curzio L. 2004. Screening and Evaluation of Materials for Microturbine Recuperators. in *Power for Land, Sea and Air, Proceedings of ASME Turbo Expo Vienna, Austria, 2004*.
20. Was G. S. 2007. *Fundamental of Materials Science for Metals and Alloy, Nuclear Engineering and Radiological Sciences*, University of Michigan: Springer Berlin Heidelberg New York, 2007.

21. Metals, A.S. and T.S. Department. 2008. *The Atlas Specialty Metals Technical Handbook of Stainless Steels* Australia: Atlas Specialty Metals Technical Services Department.
22. Li, J. and Dasgupta A., 1993. Failure-mechanism Models for Creep and Creep Rupture. *Reliability, IEEE Transactions on*, 42(3): p. 339-353.
23. Dasgupta, A. and Hu J.M. 1992. Failure Mechanism Models for Plastic Deformation. *Reliability, IEEE Transactions on*, 41(2): p. 168-174.
24. M.J.Collins, "Creep Strength in Steel and High Temperature Alloys," in *Proceeding of Meeting in University of Sheffield*, London, UK, 1972.
25. Intrater, J. and Machlin E.S., *Journal Institute of Metals* 1959. 88: p. 305.
26. Honeycombe, R.W.K., *Plastic Deformation of Metals*. 1984: Hodder Arnold.
27. Dieter G.E., *Mechanical Metallurgy*, McGraw Hill, 1988.
28. Dieter G.E., *Mechanical Metallurgy. SI Metric Edition* ed. 1988: McGraw Hill.
29. Ashby, M.F., Gandihi C., and Taplin D.M.R. 1979. Fracture Mechanism Maps and their Construction for F.C.C Metals and Alloys. *Acta Metallurgica*. 27: p. 699 - 729.
30. Maziasz, P.J. and Swindeman R. 2000. *Advanced Microturbine Systems – Program Plan for Fiscal Years 2000 – 2006*. 2000, Office of Power Technologies, Office of Energy Efficiency and Renewable Energy, U.S. Department of Energy: Washington, D.C.
31. Holdsworth, S.R., et al., Factors Influencing Creep Model Equation Selection. *International Journal of Pressure Vessels and Piping*. 85(1-2): p. 80-88.
32. Norton, F.H. 1929. *The Creep of Steels at High Temperatures*. New York: McGraw-Hill.
33. Wilshire R. B. 1985 *Creep of Metals and Alloys*. IMM North American Publication Center, vol. 5, p. 320.
34. H.Oikawa K. 1987. An Extrapolation Procedure of Creep Data. *Journal of Pressure Vessel Technology*, vol. 109, no. 1, pp. 142-146.
35. Lan C. a. I.L. 2004. Fatigue Behavior of AISI 347 Stainless Steel in Various Environments. *Journal of Materials Science*, vol. 39, no. 23, pp. 6901-6908.
36. Stinner, C. 2003. *Processing to Improve Creep and Stress Rupture Properties of Alloy T347 Foil*. Allegheny Ludlum Technical Center Internal Report: Brackenridge.

37. Laha, K., et al. 2005. Improved Creep Strength and Creep Ductility of Type 347 Austenitic Stainless Steel through the Self-Healing Effect of Boron for Creep Cavitation. *Metallurgical and Materials Transactions A*. 36(2): p. 399-409.
38. Minami, Y., Kimura H., and Tanimura M. 1985. Creep Rupture Properties of 18 Pct Cr-8 Pct Ni-Ti-Nb and Type 347H Austenitic Stainless Steels. *Journal of Materials for Energy Systems*. 7(1): p. 45-54.
39. Sasmal, B. 1997. Mechanism of the Formation of M₂₃C₆ Plates Around Undissolved NbC Particles in a Saustenitic Stainless Steel. *Journal of Materials Science*. 32(20): p. 5439-5444.
40. Lewis, M.H. and Hattersley B. 1965. Precipitation of M₂₃C₆ in Austenitic Steels. *Acta Metallurgica*. 13(11): p. 1159-1168.